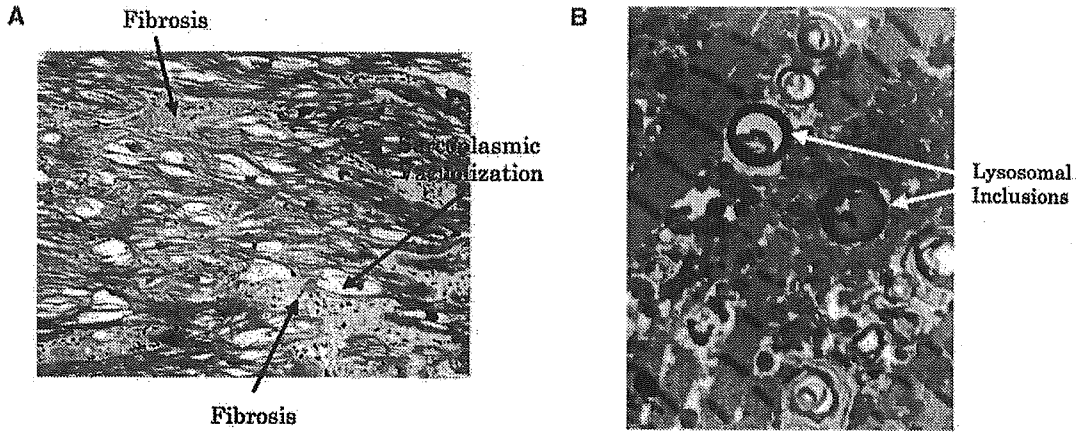

Figure 1. Histological findings of endomyocardial-biopsy specimens. A, Photomicrograph shows sarcoplasmic vacuolization of cardiac myocytes and fibrosis (hematoxylin and eosin staining). B, Electron micrograph shows typical lysosomal inclusions with a concentric lamellar configuration.

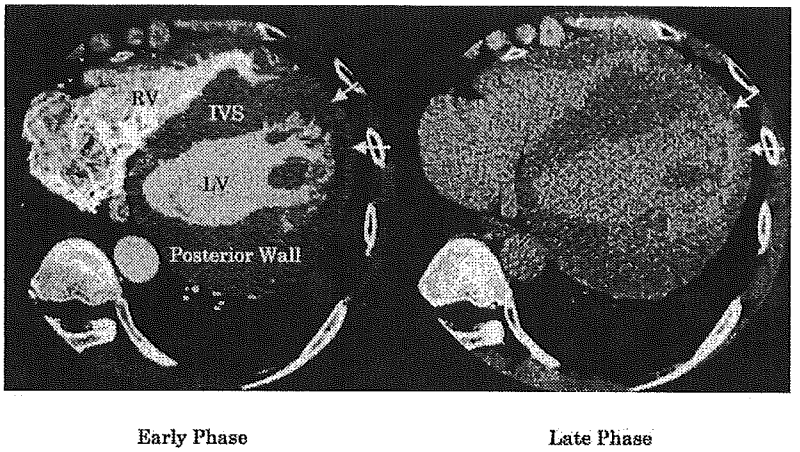

Figure 2. Axial source images of enhanced multislice computed tomography acquired 30 seconds (early phase) and 8 minutes (late phase) after the injection of the contrast material. Images show extreme hypertrophy of the interventricular septum (IVS) and posterior wall compared with the apical and lateral walls of the left ventricle (LV). The apical and lateral portions revealed lower computed tomography intensity than the IVS in the early phase (arrows). Conversely, in the late phase, the apical and lateral portions of the LV (arrows) were abnormally enhanced compared with the extremely hypertrophic IVS, suggesting more fibrotic changes in the apical and lateral myocardium. RV indicates right ventricle.

ELSEVIER

Comparative Biochemistry and Physiology Part B 135 (2003) 9–15

CBP

www.elsevier.com/locate/cbpb

Na^+/Ca^{2+} exchanger-deficient mice have disorganized myofibrils and swollen mitochondria in cardiomyocytes

Koji Wakimoto[a,*], Hisako Fujimura[a], Takahiro Iwamoto[c], Toru Oka[d], Kinji Kobayashi[b], Satomi Kita[c], Sumiyo Kudoh[d], Makoto Kuro-o[e], Yo-ichi Nabeshima[f], Munekazu Shigekawa[c], Yuji Imai[a], Issei Komuro[g]

[a]*Discovery Research Laboratory, Tanabe Seiyaku Co., Ltd, 3-16-89 Kashima, Yodogawa-ku, Osaka 532-8505, Japan*
[b]*Safety Research Laboratory, Tanabe Seiyaku Co., Ltd, 3-16-89 Kashima, Yodogawa-ku, Osaka 532-8505, Japan*
[c]*Department of Molecular Physiology, National Cardiovascular Center Research Institute, 5-7-1 Fujishiro-dai, Suita, Osaka 565-8565, Japan*
[d]*Department of Cardiovascular Medicine, University of Tokyo Graduate School of Medicine, 7-3-1 Hongo, Bunkyo-ku, Tokyo 113-8655, Japan*
[e]*Department of Pathology, University of Texas Southwestern Medical Center at Dallas, 5323 Harry Hines Boulevard, Dallas, TX 75235-9072, USA*
[f]*Department of Pathology and Tumor Biology, Graduate School of Medicine/Faculty of Medicine Kyoto University, Sakyo-ku Kyoto 606-8501, Japan*
[g]*Department of Cardiovascular Science and Medicine, Chiba University Graduate School of Medicine, Chiba, Japan*

Received 7 May 2002; received in revised form 31 December 2002; accepted 27 January 2003

Abstract

The Na^+/Ca^{2+} exchanger (NCX1) plays a key role in maintaining Ca^{2+} homeostasis in cardiomyocytes. Disruption of Ncx1 gene in mice results in embryonic lethality between embryonic day 9 and 10, with the mice lacking spontaneous heartbeats. We examined the mechanism of lack of heartbeats in Ncx1-deficient mice. Ultrastructual analysis demonstrated that Ncx1-deficient mice showed severe disorganization of myofibrils, a lack of Z-lines and swelling of mitochondria in cardiomyocytes. However, the expressions of cardiac-specific genes including transcription factor genes and contractile protein genes were not changed in Ncx1-deficient mice. Abnormal Ca^{2+} handling itself or the lack of heartbeats due to the inactivation of Ncx1 gene may cause the disorganization of myofibrillogenesis. Although NCX1 protein levels were decreased in heterozygous mice, there were no changes in NCX2 and NCX3 protein levels between wild type and heterozygous mice.

Keywords: Embryo; Heart; Heartbeat; Na^+/Ca^{2+} exchanger; NCX; Mitochondria; Mouse; Myofibril

1. Introduction

Cytosolic Ca^{2+} plays important roles in intracellular signaling in various types of animal cells, and is the main regulator of cardiac contractility. Ca^{2+} entering through the L-type Ca^{2+} channel is removed from cytosol by the sarcoplasmic reticulum Ca^{2+}-ATPase and sarcolemmal Na^+/Ca^{2+} exchanger (NCX1) in the cardiomyocytes. NCX1 serves as the main Ca^{2+} extrusion system in the heart (Bridge et al., 1990). Ncx1-deficient mice died between embryonic day 9 and 10 due to lacking heartbeats and did not show spontaneous Ca^{2+} transients in heart (Wakimoto et al., 2000).

*Corresponding author. Fax: +81-6-6300-2593.
E-mail address: wakimoto@tanabe.co.jp (K. Wakimoto).

1096-4959/03/$ - see front matter © 2003 Elsevier Science Inc. All rights reserved.
doi:10.1016/S1096-4959(03)00057-5

Recent studies have indicated that regular mechanical activity and intracellular Ca^{2+} homeostasis may have a direct effect on myofibrillogenesis in myocytes (Decker et al., 1997; Simpson et al., 1993, 1996; Schlüter et al., 1995). However, the modulatory effects of intracellular Ca^{2+} on the structural and functional characteristics of myofilaments in cardiomyocytes are less clear, because of the lack of adequate animal models. Previous studies demonstrated that a natural mutation in the Mexican axolotl (*Ambystoma mexicanum*) carries a cardiac lethal mutation in gene c (Lemanski, 1979; Lemanski et al., 1979, 2001; Zajdel et al., 1999, 2000). Hearts from the mutant embryonic Mexican axolotl failed to beat and did not form organized myofibrils. Although the protein coded by gene c has not yet been clarified, lack of heartbeats in the mutant embryonic Mexican axolotl is similar to that of Ncx1-deficient mice. This mutant Mexican axolotl suggests that contraction of heart muscle requires a precise organization of contractile proteins. In the present study, we examined the ultrastructural changes in cardiomyocytes to investigate the effects of the lack of NCX1 in myofibrillogenesis.

2. Materials and methods

2.1. Reverse transcription-polymerase chain reaction (RT-PCR)

RNAs of wild type ($Ncx1^{+/+}$), heterozygous ($Ncx1^{+/-}$) and homozygous ($Ncx1^{-/-}$) mutant mice embryos were isolated and copied into cDNA by SUPERSCRIPT II RNaseH(−) reverse transcriptase (Gibco BRL) according to manufacturer's recommendations. PCR was performed using the synthesized cDNA as a template and pairs of primers expected to amplify the cardiac-specific genes (Table 1). The cardiac-specific genes examined in this study were: the cardiac-specific transcription factors, Csx/Nkx2.5 and GATA-4, atrial natriuretic peptide (ANP), and the ventricular isoform of myosin light chain (MLC2v). The cycling conditions were 3 min at 94 °C for the initial denaturation step followed by 40 cycles of 1 min at 94 °C (denaturation), 1 min at 55 °C (annealing), and 1 min at 72 °C (elongation) using a DNA Thermal Cycler (Perkin Elmer). The PCR products were electrophoresed on 2% agarose gel; stained by ethidium bromide and photographed on Fuji instant film FP-3000B (Fuji Film, Japan).

2.2. Ultrastructual analysis in cardiomyocytes

Whole embryos at day 9.5 were fixed with 2% paraformaldehyde and 2.5% glutaraldehyde in 0.1 M phosphate buffer (pH 7.3), and post-fixed with 1% osmium tetraoxide in phosphate buffer (pH 7.3). After dehydration, specimens were embedded in Epon-Araldite. Semi-thin sections and ultrathin sections were stained with toluidine blue, and uranyl acetate and lead citrate, respectively. Ultrathin sections were examined with a transmission electron microscope (JEM-1210).

2.3. Western blot analysis

Western blot analysis was performed as described previously (Iwamoto et al., 1998). Briefly, polyclonal antibodies against NCX isoforms were used, which were raised by immunizing rabbits with maltose-binding protein, fusion proteins or glutathione *S*-transferase fusion proteins containing either amino acids 240-737 of NCX1, amino acids 281-637 of NCX2, or amino acids 275–637 of NCX3. The proteins (100 μg/lane) from adult $Ncx1^{+/+}$ and $Ncx1^{+/-}$ mice (15 week old) were subjected to SDS-PAGE on a 7.5% gel and then blotted to the immobilon membranes (Bio-Rad). The proteins on the membranes were immunostained with polyclonal antibodies and visualized using the ECL detection system (Amersham).

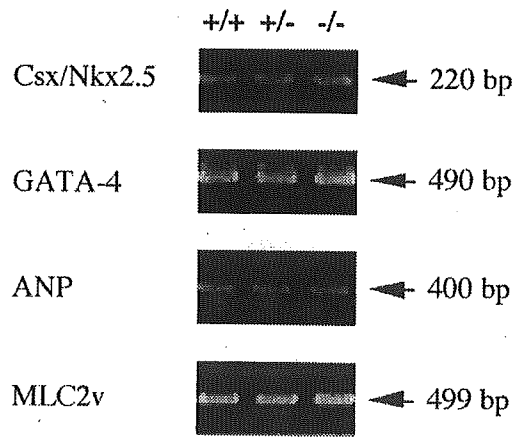

Fig. 1. RT-PCR analysis of cardiac-specific genes in Ncx1-deficient mice embryos at day 9.5, Specific primers for Csx/Nkx2.5, GATA-4, ANP, and MLC2v were used.

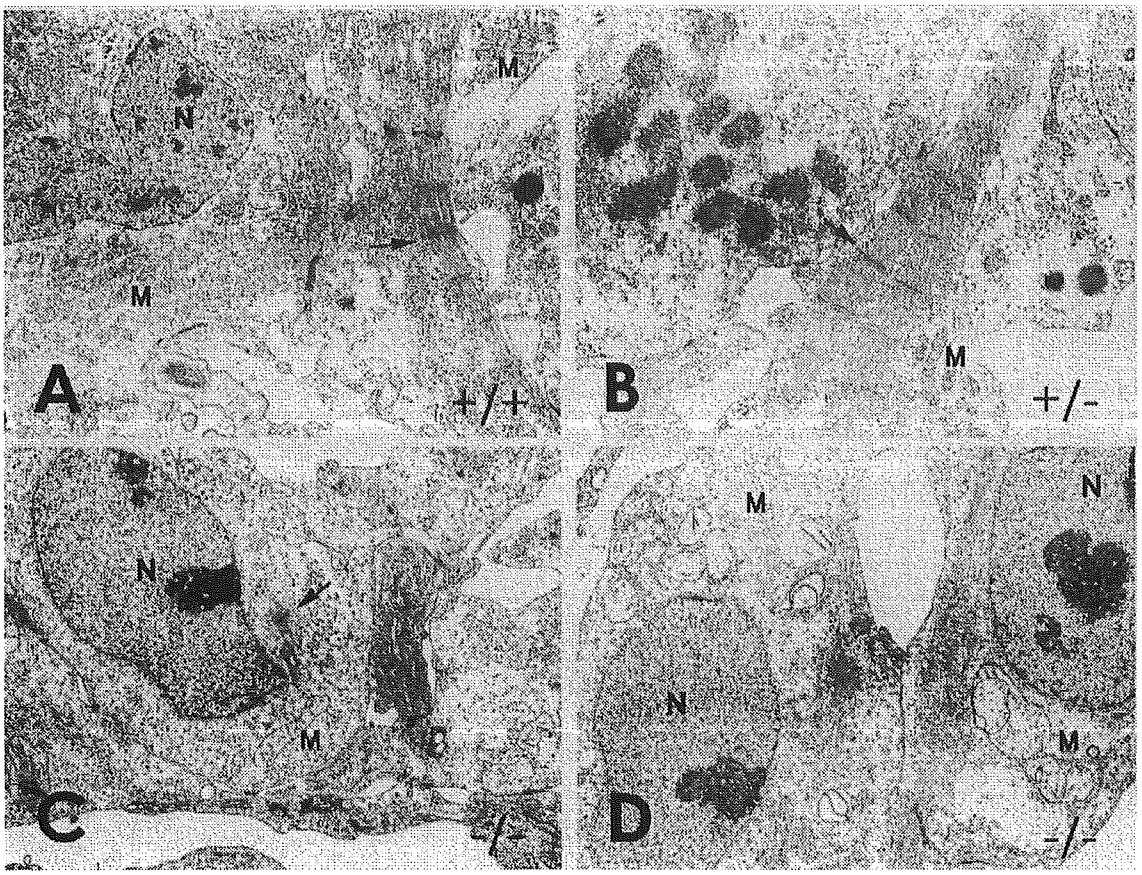

Fig. 2. Ultrastructual analysis of cardiomyocytes in Ncx1-deficient mice embryos at day 9.5. Myofibrils are parallel and sarcomere bands that are well developed in $Ncx1^{+/+}$ (a) and $Ncx1^{+/-}$ (b) mice. No (d) or single (c) Z-line are found in $Ncx1^{-/-}$ mice. Although normal mitochondrias are found in $Ncx1^{+/+}$ and $Ncx1^{+/-}$ mice, swollen mitochondria are found in $Ncx1^{-/-}$ mice. Arrows indicate Z-lines, N – nucleus, M – mitochondria. Similar results were obtained in three independent experiments.

3. Results

3.1. Cardiac-specific gene expression in $Ncx1^{-/-}$ mice

To elucidate the affects of NCX1 on the expression of cardiac genes, we performed RT-PCR using specific oligonucleotide primers (Table 1). Total RNA from $Ncx1^{+/+}$, $Ncx1^{+/-}$, and $Ncx1^{-/-}$ mice of day 9.5 were used. The expression of cardiac transcription factor genes, such as Csx/Nkx2.5 and GATA-4 was not affected by the absence of Ncx1 gene (Fig. 1). These results indicate that expression of the cardiac-specific

Table 1
Oligonucleotide primers for cardiac-specific genes

Gene	5′-primer	3′-primer	Size of PCR product (bp)
Csx/Nkx2.5	5′-TCTCCGATCCATCCCACTTTATTG-3′	5′-TTGCGTTACGCACTCACTTTAATG-3′	220
GATA-4	5′-GCACAGCCTGCCTGGACG-3′	5′-GCTGCTGCTGCTGCTAGTGG-3′	490
ANP	5′-CTCTGAGAGCGGCAGTGCT-3′	5′-TATGCAGAGTGGGAGAGGCA-3′	400
MLC2v	5′-GCCAAGAAGCGGATAGAAGG-3′	5′-CTGTGGTTCAGGGCTCAGTC-3′	499

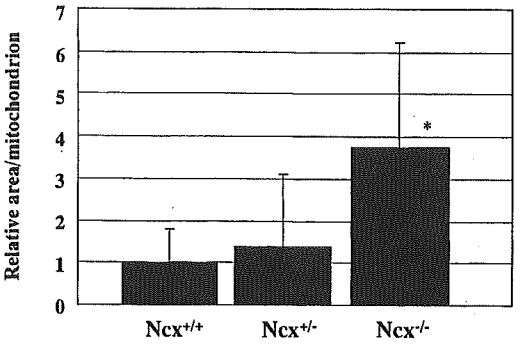

Fig. 3. Relative areas of cross sections per mitochondrion are presented as ratio of the value for $Ncx^{+/+}$. Data represent mean ± S.E. ($n=8$). Significant difference between groups was evaluated using unpaired Student's t-test. Probability less than 5% ($P<0.05$) was considered to be statistically significant. $^{*}P<0.05$ vs. $Ncx^{+/+}$ and $Ncx^{+/-}$.

transcription factor is not dependent on Ncx1 gene, and suggests that cardiac development is not impaired in $Ncx1^{-/-}$ mice. Furthermore, the expression levels of both a cardiac-specific hormonal gene ANP and a contractile protein gene MLC2v were not changed in $Ncx1^{-/-}$ mice compared with $Ncx1^{+/+}$ mice embryos at day 9.5 (Fig. 1).

3.2. Ultrastructual changes in cardiomyocytes at day 9.5 embryos

To investigate the cause of defects in heartbeats, we next examined the ultrastructure of cardiomyocytes at embryonic day 9.5. Electronmicroscopic studies showed that abundant myofilaments were present in the cardiomyocytes in $Ncx1^{+/+}$ and $Ncx1^{+/-}$ mice (Fig. 2a and b). Myofibrillar organization showed the usual sarcomeric pattern with a regular myofilament arrangement. Desmosomes or intercalated disks were also present. In contrast, cardiomyocytes in $Ncx1^{-/-}$ mice showed severe disorganization of myofibrils (Fig. 2c and d). Myofilaments were distributed at random or aligned with Z-line. Reduced myofilament bundles formed no or single Z-lines, and intercalated-disk-like structures were present, associated with myofilament bundles, which had no Z-lines. In addition, mitochondria were swollen (Fig. 2 and Fig. 3), and irregular in shape with low electron-dense matrix and dilated cristae.

3.3. Western blot analysis

To investigate the protein level in adult $Ncx1^{+/-}$ mice, we performed Western blot analysis. In $Ncx1^{+/-}$ mice, NCX1 protein levels were significantly reduced in heart, kidney and brain. Especially, in heart and kidney, the protein levels of NCX1 in $Ncx1^{+/-}$ mice were approximately half of those of $Ncx1^{+/+}$ mice (Fig. 4a). Furthermore, we examined whether the NCX2 and NCX3 protein levels were up regulated to compensate for the reduced NCX1 protein. NCX2 and NCX3 mRNA are expressed in brain. As shown in Fig. 4b, there was no difference in NCX2 and NCX3 protein levels in brain between $Ncx1^{+/+}$ and $Ncx1^{+/-}$ mice, suggesting that the reduction of NCX1 proteins could not induce the expression of NCX2 and NCX3 proteins in brain.

4. Discussion

To date, three Ncx genes (Ncx1, Ncx2 and Ncx3) have been cloned and reported to be coded by distinct genes in mammals (Nicoll et al., 1990, 1996; Li et al., 1994). We have generated NCX deficient mice by disrupting the locus of Ncx1 (Wakimoto et al., 2000). The $Ncx1^{-/-}$ mice died between embryonic day 9 and 10. Their hearts did not beat and cardiomyocytes showed apoptosis. After we had reported the Ncx1-deficient mice, two groups subsequently reported the same mutant mice. Cho et al. (2000) demonstrated that $Ncx1^{-/-}$ mice died before embryonic day 10.5, and that their myocardial cells showed apoptosis. Their results were in good agreement with our previous results. However, Koushik et al. (2001) reported that their mutant mice had some differences from our mutant mice. They indicated that $Ncx1^{-/-}$ mice were alive until embryonic day 11.0 and did not show apoptosis in the heart. However, their staging of mouse embryos seemed to be different from ours. For example, mutant mice which they designated embryonic day 9.0, did not close the neural tubes, suggesting that the mice might be instead approximately at embryonic day 8.0 (Rugh, 1990). Koushik et al. (2001) also demonstrated that NCX1 protein levels were unaltered between $Ncx1^{+/+}$ and $Ncx1^{+/-}$ mice. In this study, we showed that protein levels of NCX1 were reduced in the hearts, kidneys and brains of our $Ncx1^{+/-}$ mice. We also reported that NCX1 protein levels in aortic smooth muscles were

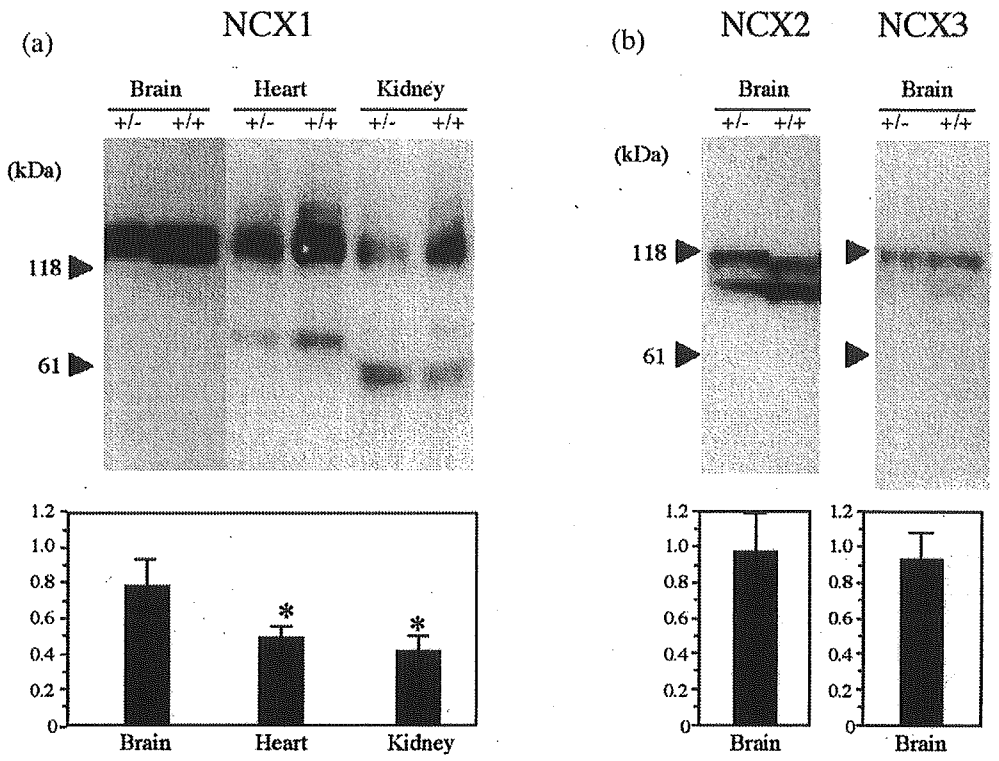

Fig. 4. Western blot analyses of heart, kidney, and brain in adult $Ncx1^{+/+}$ and $Ncx1^{+/-}$ mice. The molecular mass markers are shown on the left. Densitometric estimates of the protein in $Ncx1^{+/-}$ mice are presented as ratio of the value for that in $Ncx1^{+/+}$ mice (lower panel). Each column and bar represents mean±S.E. ($n=8$). Significant difference between groups was evaluated using unpaired Student's t-test. Probability less than 5% ($P<0.05$) was considered to be statistically significant. The NCX1 protein levels in $Ncx1^{+/-}$ mice are lower than those in $Ncx1^{+/+}$ mice (a), while the NCX2 and NCX3 protein levels are not changed between $Ncx1^{+/+}$ and $Ncx1^{+/-}$ mice (b).

reduced in $Ncx1^{+/-}$ mice (Wakimoto et al., 2000). These results were consistent with the results that the Na^+/Ca^{2+} exchange activity was down-regulated in cultured smooth muscle cells of $Ncx1^{+/-}$ mice, and that tension development of the aortic ring was impaired in $Ncx1^{+/-}$ mice (Wakimoto et al., 2000). As for apoptosis in the heart and the protein levels in $Ncx1^{+/-}$ mice, it may be due to the different genetic backgrounds.

In this study, we demonstrated that $Ncx1^{-/-}$ mice have disorganized myofibrils and swollen mitochondria in the cardiomyocytes. Our results are in good agreement with those of Koushik et al. (2001) on this point, although they did not mention the abnormality of mitochondria. Mitochondria that are exposed to high concentrations of Ca^{2+} have megachannels in their inner mitochondrial membranes that are open (Haworth and Hunter, 1979). This event, also named the mitochondria permeability transition (MPT), is considered to be an early event in apoptosis in some cells and possibly a trigger of cell death in ischemia/reperfuison injury (Marchetti et al., 1996; Kroemer, 1997; Griffiths and Halestrap, 1993; Uchino et al., 1995). Since $Ncx1^{-/-}$ mice lack heartbeats and the main extrusion system of Ca^{2+} from cells, the hearts of $Ncx1^{-/-}$ mice are considered to be under ischemic conditions due to lack of blood circulation. These pathological conditions might induce the swelling of mitochondria. RT-PCR analysis revealed that cardiac functional and structural genes were not affected by the lack of Ncx1 gene in the transcriptional level (Fig. 1). Therefore, the disorganized myofibrils in $Ncx1^{-/-}$ mice are thought to be induced by the lack of contractile activity or abnormal intracellu-

lar Ca^{2+} concentration. It is not clear which contributes to disruption of myofibrillogenesis, the lack of contractile activity or abnormal Ca^{2+} signaling. Recent studies have demonstrated the important roles of contractile activity in myofibrillogenesis (Simpson et al., 1996; Samarel and Engelmann, 1991; Samarel et al., 1992; Sharp et al., 1993). Sharp et al. (1993) showed that the inhibition of contractile activity by L-type Ca^{2+} channel antagonists led to disruption of actin filaments of myofibrils, and that active tension development was critical to the maintenance of filamentous actin structure in neonatal cardiomyocytes. In contrast, Horackova et al. (2000) reported that the inhibition of contractile activity by verapamil or nifedipine had very little effect on the myofibrillar arrangement in adult guinea pig cardiomyocytes. They clearly demonstrated that the ultrastructure of the regularly assembled myofilaments and myofibrils was not changed, even after the cardiomyocytes had been quiescent for 72 h. These results in adult cardiomyocytes are quite different from those by Sharp et al. (1993) in neonatal cardiomyocytes. Horackova et al. (2000) also demonstrated that the inhibition of NCX1 caused complete fragmentation of both actin and the myosin filaments and the inhibition of contractile activity in adult cardiomyocytes. They described that contractile inactivity did not have major effects on the structural and biochemical characteristics of the myofilaments, and that maintenance of the normal functional properties of cardiomyocytes was mostly dependent on the proper functioning of Ca^{2+} extrusion from the cells via NCX1. During the neonatal period, when the sarcoplasmic reticulum was poorly developed structurally and functionally, cardiac contraction and relaxation were more dependent on Ca^{2+} fluxes across the sarcolemma, than in adults of most mammalian species (Mahony, 1996). Therefore, the lack of contractility as well as abnormal Ca^{2+} handling may cause impaired myofibrillogenesis in the embryo of $Ncx^{-/-}$ mice.

Acknowledgments

We thank M. Kurabe and Y. Hamasaki for their technical support. We are grateful to A. Nishida, N. Yanaka, and H. Imahie for their helpful discussions, and S. Nito for his continuous kindness.

References

Bridge, J.H., Smolley, J.R., Spitzer, K.W., 1990. The relationship between charge movements associated with ICa and INa-Ca in cardiac myocytes. Science 248, 376–378.

Cho, C.-H., Kim, S.S., Jeong, M.-J., Lee, C.O., Shin, H.-S., 2000. The Na^+–Ca^{2+} exchanger is essential for embryonic heart development in mice. Mol. Cells 10, 712–722.

Decker, M.L., Janes, D.M., Barclay, M.M., Harger, L., Decker, R.S., 1997. Regulation of adult cardiocyte growth: effects of active and passive mechanical loading. Am. J. Physiol. 272, H2902–2918.

Griffiths, E.J., Halestrap, A.P., 1993. Protection by Cyclosporin A of ischemia/reperfusion-induced damage in isolated rat hearts. J. Mol. Cell Cardiol. 25, 1461–1469.

Haworth, R.A., Hunter, D.R., 1979. The Ca^{2+}-induced membrane transition in mitochondria. II. Nature of the Ca^{2+} trigger site. Arch. Biochem. Biophys. 195, 460–467.

Horackova, M., Morash, B., Byczko, Z., 2000. Altered transarcolemmal Ca transport modifies the myofibrillar ultrastructure and protein metabolism in cultured adult ventricular cardiomyocytes. Mol. Cell Biochem. 204, 21–33.

Iwamoto, T., Pan, Y., Nakamura, T.Y., Wakabayashi, S., Shigekawa, M., 1998. Protein kinase C-dependent regulation of Na^+/Ca^{2+} exchanger isoforms NCX1 and NCX3 does not require their direct phosphorylation. Biochemistry 37, 17230–17238.

Koushik, S.V., Wang, J., Rogers, R., Moskophidis, D., Lambert, N.A., Creazzo, T.L., et al., 2001. Targeted inactivation of the sodium-calcium exchanger (Ncx1) results in the lack of a heartbeat and abnormal myofibrillar organization. FASEB J. 15, 1209–1211.

Kroemer, G., 1997. The proto-oncogene Bcl-2 and its role in regulating apoptosis. Nat. Med. 3, 614–620.

Lemanski, L.F., 1979. Role of tropomyosin in actin filament formation in embryonic salamander heart cells. J. Cell Biol. 82, 227–238.

Lemanski, L.F., Paulson, D.H., Hill, C.S., 1979. Normal anterior endoderm corrects the heart defect in cardiac mutant salamanders. Science 204, 860–862 *Ambystoma mexicanum*.

Lemanski, L.F., Meng, F., Lemanski, S.L., Dawson, N., Zhang, C., Foster, D., et al., 2001. Creation of chimeric mutant axolotls: a model to study early embryonic heart development in Mexican axolotls. Anat. Embryol. 203, 335–342 Berl.

Li, Z., Matsuoka, S., Hryshko, L.V., Nicoll, D.A., Bersohn, M.M., Burke, E.P., et al., 1994. Cloning of the NCX2 isoform of the plasma membrane Na^+–Ca^{2+} exchanger. J. Biol. Chem. 269, 17434–17439.

Mahony, L., 1996. Regulation of intracellular calcium concentration in the developing heart. Cardiovasc. Res. 31, E61–E67.

Marchetti, P., Castedo, M., Susin, S.A., Zamzami, N., Hirsh, T., Macho, A., et al., 1996. Mitochondrial permeability transition is a central coordinating event of apoptosis. J. Exp. Med. 184, 1155–1160.

Nicoll, D.A., Longoni, S., Philipson, K.D., 1990. Molecular cloning and functional expression of the cardiac sarcolemmal Na^+–Ca^{2+} exchanger. Science 250, 562–565.

Nicoll, D.A., Quednau, B.D., Qui, Z., Xia, Y., Lusis, A.J.,

Philipson, K.D., 1996. Cloning of a third mammalian Na^+–Ca^{2+} exchanger, NCX3. J. Biol. Chem. 271, 24914–24921.

Rugh, R., 1990. The Mouse — Its Reproduction and Development. Oxford University Press.

Samarel, A.M., Engelmann, G.L., 1991. Contractile activity modulates myosin heavy chain-beta expression in neonatal rat heart cells. Am. J. Physiol. 261, H1067–H1077.

Samarel, A.M., Spragia, M.L., Maloney, V., Kamal, S.A., Engelmann, G.L., 1992. Contractile arrest accelerates myosin heavy chain degradation in neonatal rat heart cells. Am. J. Physiol. 263, C642–C652.

Schlüter, K.-D., Millar, B.C., McDermott, B.J., Piper, H.M., 1995. Regulation of protein synthesis and degradation in adult ventricular cardiomyocytes. Am. J. Physiol. 269, C1347–C1355.

Sharp, W.W., Terracio, L., Borg, T.K., Samarel, A.M., 1993. Contractile activity modulates actin synthesis and turnover in cultured neonatal rat heart cells. Circ. Res. 73, 172–183.

Simpson, D.G., Decker, M.L., Clark, R.S., Decker, R.S., 1993. Contractile activity and cell-cell contact regulate myofibrillar organization in cultured cardiac myocytes. J. Cell Biol. 123, 323–336.

Simpson, D.G., Sharp, W.W., Borg, T.K., Price, R.L., Terracio, P.L., Samarel, A.M., 1996. Mechanical regulation of cardiac myocyte protein turnover and myofibrillar structure. Am. J. Physiol. 270, C1075–C1087.

Uchino, H., Elmer, E., Uchino, K., Lindvall, O., Siesjo, B.K., 1995. Cyclosporin A dramatically ameliorates CA1 hippocampal damage following transient forebrain ischaemia in the rat. Acta. Physiol. Scand. 155, 469–471.

Wakimoto, K., Kobayashi, K., Kuro-o, M., Yao, A., Iwamoto, T., Yanaka, N., et al., 2000. Targeted disruption of Na^+/Ca^{2+} exchanger gene leads to cardiomyocytes apoptosis and defects in heartbeat. J. Biol. Chem. 275, 36991–36998.

Zajdel, R.W., Dube, D.K., Lemanski, L.F., 1999. The cardiac mutant Mexican axolotl is a unique animal model for evaluation of cardiac myofibrillogenesis. Exp. Cell Res. 248, 557–566.

Zajdel, R.W., McLean, M.D., Isitmangil, G., Lemanski, L.F., Wieczorek, D.F., Dube, D.K., 2000. Alteration of cardiac myofibrillogenesis by liposome-mediated delivery of exogenous proteins and nucleic acids into whole embryonic hearts. Anat. Embryol. 201, 217–228 Berl.

Available online at www.sciencedirect.com
SCIENCE DIRECT®
Life Sciences 73 (2003) 917–932
Life Sciences
www.elsevier.com/locate/lifescie

Characterization of a novel *C. elegans* RGS protein with a C2 domain: evidence for direct association between C2 domain and Gαq subunit

Motoko Sato[a,b], Kayoko Moroi[a], Mariko Nishiyama[a], Jing Zhou[a], Hirokazu Usui[a,c], Yoshitoshi Kasuya[a], Mitsunori Fukuda[d], Yuji Kohara[e], Issei Komuro[b], Sadao Kimura[a,*]

[a] *Department of Biochemistry and Molecular Pharmacology, Chiba University Graduate School of Medicine, 1-8-1 Inohana Chuo-ku, Chiba 260-8670, Japan*
[b] *Department of Cardiovascular Science and Medicine, Chiba University Graduate School of Medicine, Chiba 260-8670, Japan*
[c] *Department of Reproductive Medicine, Chiba University Graduate School of Medicine, Chiba 260-8670, Japan*
[d] *The Fukuda Initiative Research Unit, RIKEN (Institute of Physical and Chemical Research), Wako 351-0198, Japan*
[e] *Genome Biology Laboratory, National Institute of Genetics, Mishima 411-8540, Japan*

Received 4 November 2002; accepted 7 February 2003

Abstract

RGS (regulator of G protein signaling) proteins are GTPase-activating proteins (GAPs) for heterotrimeric G protein α subunits and negatively regulate G protein-mediated signal transduction. In this study, we determined the cDNA sequence of a novel *Caenorhabditis elegans* (*C. elegans*) RGS protein. The predicted protein, termed C2-RGS, consists of 782 amino acids, and contains a C2 domain and an RGS domain. C2 domains are typically known to be Ca^{2+} and phospholipid binding sites, found in many proteins involved in membrane traffic or signal transduction, and most of their biological roles are not identified. To study the function of C2-RGS protein, a series of six truncated versions of C2-RGS were constructed. When the full-length protein of C2-RGS was expressed transiently in AT1a-293T cells, ET-1-induced Ca^{2+} responses were strongly suppressed. When each of the mutants with either RGS domain or C2 domain was expressed, the Ca^{2+} responses were suppressed moderately. Furthermore, we found that C2 domain of PLC-β1 also had a similar moderate inhibitory effect. RGS domain of C2-RGS bound to mammalian and *C. elegans* Gαi/o and Gαq subunits only in the presence of GDP/AlF_4^-, and had GAP activity to Gαi3. On the other hand, C2 domains of C2-RGS and PLC-β1 also bound strongly to Gαq subunit, in the presence of GDP, GDP/AlF_4^-, and GTPγS, suggesting the stable persistent association between these C2 domains and Gαq subunit at any stage during GTPase cycle. These results indicate that both the RGS

* Corresponding author. Tel.: +81-43-226-2194; fax: +81-43-226-2196.
E-mail address: s-kimura@faculty.chiba-u.jp (S. Kimura).

0024-3205/03/$ - see front matter
doi:10.1016/S0024-3205(03)00355-2

domain and the C2 domain are responsible for the inhibitory effect of the full-length C2-RGS protein on Gαq-mediated signaling, and suggest that C2 domains of C2-RGS and PLC-β1 may act as a scaffold module to organize Gαq and the respective whole protein molecule in a stable signaling complex, both in the absence and presence of stimulus.

Keywords: *Caenorhabditis elegans*; RGS; C2 domain; G protein; Scaffold

Introduction

A variety of hormones, neurotransmitters, and physical stimuli, such as light, exert their actions by activating G protein-coupled receptors (GPCRs). It is greatly important to regulate adequately the intracellular signalings mediated by heterotrimeric G proteins. Recent genetic and biochemical studies have revealed the existence of a novel family of proteins termed "regulators of G protein signaling" (RGS) that act as GTPase-activating proteins (GAPs) for heterotrimeric G protein α subunits and negatively regulate G protein-mediated signal transduction (Zheng et al., 1999; De Vries et al., 2000; Ross and Wilkie, 2000). RGS proteins contain a conserved 120 amino acids domain (RGS domain), which is responsible for binding to Gα subunits and accelerating GTP hydrolysis by Gα to turn off signaling (Hepler et al., 1997). Most of them have been shown to act as GAPs toward Gαi/o and/or Gαq/11, but not Gαs (Zheng et al., 1999).

Since the discovery of Sst2, an RGS protein in *Saccharomyces cerevisiae* (Dohlman et al., 1996), EGL-10 in *Caenorhabditis elegans* (*C. elegans*) (Koelle and Horvitz, 1996), and GAIP in humans (De Vries et al., 1995), RGS proteins have been identified in a wide range of species, from yeast to human, including over 20 mammalian RGS proteins (Ross and Wilkie, 2000). Some RGS proteins consist predominantly of an RGS domain, while others posses an RGS domain along with additional domains (De Vries et al., 2000; Ross and Wilkie, 2000). Based on the complete sequence of *C. elegans* genome published in 1998 (The C. elegans Sequencing Consortium, 1998), the presence of a novel RGS protein was suggested by using the computer software, GENE FINDER. This protein, termed C2-RGS, was predicted to have a C2 domain in the N-terminal, in addition to the RGS domain in the C-terminal.

C2 domain, which consists of about 130 amino acids, was originally defined as a homologous domain to the C2 regulatory region of mammalian Ca^{2+}-dependent protein kinase C (PKC) isoforms α, β, and γ (Nishizuka, 1988). It has been identified in various signaling molecules (Rizo and Sudhof, 1998; Nalefski and Falke, 1996), including proteins involved in signal transduction (e.g. phospholipases C (PLC) and protein kinase C (PKC)), those involved in membrane trafficking (e.g. synaptotagmins and Doc2s), ubiquitination enzymes and GTPase-activating proteins (Brose et al., 1992; Sutton et al., 1995; Li et al., 1995; Ponting and Parker, 1996; Fukuda and Mikoshiba, 2000; Fukuda et al., 2001). C2 domains are composed of a common eight-stranded antiparallel β-sandwich consisting of four-stranded β-sheets, although their structures have been classified into two groups based on their topology (e.g. synaptotagmin I C2A domain with type I topology and PLC-δ1 C2 domain with type II topology) (Nalefski and Falke, 1996). C2 domain is typically known as a Ca^{2+}/phospholipid binding motif (Rizo and Sudhof, 1998). However, all C2 domains are not obligatory Ca^{2+} and phospholipids binding domains. They have diverged evolutionally into Ca^{2+}-dependent and Ca^{2+}-independent forms that interact with multiple targets, and functions of C2 domains of the Ca^{2+}-independent type remain largely unknown.

If the RGS domain of C2-RGS is functionally similar to those of known mammalian RGS proteins, it is likely that C2-RGS protein can suppress G protein signaling. On the other hand, the C2 domain may also have some unknown functions in the intracellular signal transduction. Moreover, if the C2 domain might somehow influence the function of the RGS domain, or vice versa, it is possible that the total function of C2-RGS protein might be tuned more finely, or more efficiently, by mutual contribution of these two domains. In fact, in some cases of RGS proteins with multiple domains, their RGS functions are often activated by cooperation of the intramolecular domains other than the RGS domains. For example, Gγ subunit-like (GGL) domains in RGS7 and RGS9 can enhance the RGS functions by their specific interactions with Gβ5 (Kovoor et al., 2000). On the other hand, p115RhoGEF, a guanine nucleotide exchanging factor (GEF) specific for Rho, contains an RGS domain, which acts as a GAP for Gα12 and Gα13, in addition to a dbl homology (DH) domain, which is responsible for the GEF activity. The RGS domain in p115RhoGEF is considered to function to link Gα13 to Rho so that Gα13 can activate Rho through the DH domain (Hart et al., 1998; Kozasa et al., 1998). Furthermore, in the case of G protein-coupled receptor kinase 2 (GRK2) which has an RGS domain, a kinase domain, and a PH domain, the inhibitory effect of GRK2 on Gαq/11-mediated signaling owes not only to phosphorylation of activated receptors by the kinase domain, but also to specific interaction between the RGS domain and Gαq/11 subunits (Carman et al., 1999; Usui et al., 2000).

The present study was performed to clarify the function of C2-RGS protein and roles of the C2 domain and the RGS domain in G protein signaling. Functional studies with the full-length C2-RGS protein and the various mutants showed that the full-length protein suppressed potently intracellular Ca^{2+} responses induced by endothelin–1 (ET-1), and that not only RGS domain, but also C2 domain of C2-RGS protein suppressed the responses moderately, suggesting synergistic actions of these two domains. Binding experiments also demonstrated direct biochemical interaction between the C2 domain and Gαq subunit, in addition to the binding of the RGS domain to Gαq and Gαi/o subunits. Thus, we propose in this study a novel functional role of some C2 domains in Gαq-mediated intracellular signal transduction.

Methods

Materials

Dulbecco's modified Eagle's medium (DMEM), Lipofectamine Reagent and Plus Reagent were from Invitrogen. pQE30, *E. coli* strain M15, Ni^{2+}-NTA agarose, and mouse anti-His_6 antibody (Ab) were from Qiagen. Glutathione-sepharose was from Amersham Biosciences. A cocktail of protease inhibitors, Complete™ was from Roche Diagnostics. Fura-2/AM was from Dojin Chemicals Institute Co. Endothelin-1 (ET-1) were from Peptide Institute. Chemiluminescence reagent, rabbit anti-Gαs Ab, and anti-Gαq/11 Ab were from Perkin Elmer Instruments. Rabbit anti-Gαi3, mouse anti-GST, and mouse anti-c-myc Abs were from Santa Cruz Biotechnology. Rabbit anti-Gαi2 and Gαo Abs were kindly provided by Dr. T. Asano (Aichi Human Service Center). Peroxidase-conjugated goat anti-mouse and anti-rabbit IgG Abs were from Kirkegoard Perry Laboratories. Plasmids of G protein α subunits (rat Gαs, rat Gαi3, rat Gαo and mouse Gαq) were kindly provided by Dr. T. Sakurai (University of Tsukuba).

Sequencing of C2-RGS cDNA

A cDNA clone of F56B6, yk534f10 encoding C2-RGS protein originated from the Y. Kohara EST project for *C. elegans* (National Institute of Genetics, Japan). Full-length cDNA sequence of C2-RGS protein was determined with ABI PRISM™ 377 DNA sequencing system (PE Biosystems).

Plasmid Construction

cDNAs encoding the full-length C2-RGS, EGL-30 (*C. elegans* homologue of Gαq, 82% identical to human Gαq), and GOA-1 (*C. elegans* homologue of Gαo, 82% identical to human Gαo) were obtained from EST clones (yk534f10, yk361c6, and yk213d9, respectively, prepared by the Y. Kohara EST project). RGS domain (RGS: amino acid residues 632–763) of C2-RGS, a long fragment of C2 domain (C2L: amino acid residues 253–436), a short fragment of C2 domain (C2S: amino acid residues 271–388), C2 domain of human PLC-β1 (PLC-C2: amino acid residues 674–800) were constructed by polymerase chain reaction (PCR). cDNAs encoding C2-RGS, RGS, C2L, C2S, PLC-C2, EGL-30 and GOA-1, were subcloned into pCMV6c with the coding sequence for c-myc or c-myc-GST epitope tag at the N-terminal of the multi-cloning sites.

The C2 domain-deleted mutant (ΔC2) was constructed by following methods; In order to delete the sequence corresponding to C2 domain (nucleotides 809 −1167) from pCMV6c-C2-RGS plasmid, a cDNA fragment of C2-RGS (nucleotides 1-808) with the upstream short sequence of pCMV6c and another fragment (nucleotides 1168–1782) were generated by PCR using primers with *Pvu*II/*Nco*I and *Nco*I/*Pvu*II restriction enzyme sites, respectively. Then, the two fragments were ligated with pCMV6c-C2-RGS plasmid, which was digested by *Pvu*II. Similarly, the RGS domain-deleted mutant (ΔRGS) was constructed by deleting the sequence corresponding to RGS domain (nucleotides 1933–2289) from pCMV6c-C2-RGS plasmid. A fragment of C2-RGS (nucleotides 1675–1932) and another fragment (nucleotides from 2290 to 2349 (the end nucleotide)) of C2RGS with the downstream short sequence of pCMV6c were generated by PCR using primers with *Acc*I /*Nco*I and *Nco*I/*Acc*I restriction enzyme sites. The two PCR fragments were ligated with pCMV6c-C2-RGS plasmid, which was digested by *Acc*I. To generate the mutant lacking both C2 and RGS domains (ΔC2ΔRGS), a C2-deletion fragment (nucleotides 1-1601) was cut down from pCMV6c-ΔC2 plasmid using *Xba*I and *Nru*I, and the corresponding part of pCMV6c-ΔRGS plasmid was replaced by it.

The construction of mammalian expression vectors containing cDNAs encoding c-myc-tagged human RGS5 and N-terminal hexahistidine (His_6)-tagged mouse Gαq was described previously (Usui et al., 2000). cDNAs encoding RGS domain of C2-RGS, human RGS5, and rat Gαi3, were inserted in pQE30, for generating the His_6-tagged proteins. DNA sequences of all vectors were confirmed using ABI PRISM™ 377 DNA sequencing system (PE Biosystems).

Cell line, cell culture and transfection

AT1a-293T cells (293T cells stably expressing hemagglutinin (HA)-tagged mouse angiotensin AT1a receptor) were maintained at 37 °C in a humidified atmosphere of 5% CO_2 − 95% air in DMEM containing 100 μg/ml of hygromycin B and 10% fetal bovine serum. Cells were transfected with vectors containing various forms of C2-RGS or the empty vector (pCMV6c) using Lipofectamine reagent and Plus reagent, and used for experiments after 24 h.

Measurement of intracellular calcium ([Ca^{2+}]i) transient

Cells were incubated in the loading buffer [20 mM HEPES-Hanks (pH 7.4) containing 11 mM glucose and 0.1% bovine serum albumin] with 4 μM Fura-2/AM for 40 min at 37 °C. Intracellular Ca^{2+} transients evoked by ET-1 were monitored by a CAF-110 fluorescence spectrophotometer (Jasco Co.) or FDSS3000 (Hamamatsu Photonics K.K.) with dual excitation at 340 nm/380 nm and emission at 500 nm. Then these cells were harvested and the expression levels of C2-RGS, its mutants, or C2 domain of PLC-β1 were checked by subsequent SDS-PAGE and immunoblotting using anti-c-myc Ab followed by peroxidase-conjugated goat anti-mouse IgG Ab as described below.

Expression and purification of His_6-tagged RGS domain protein

His_6-tagged RGS domain of C2-RGS protein, human RGS5 and rat Gαi3, were purified from *E. coli* strain M15, using Ni^{2+}-NTA agarose beads according to the manufacturer's instructions. Each of the purified proteins showed a single band on SDS-PAGE and was used for binding experiments.

Binding experiments of His_6-RGS and Gα subunits

Membranes were prepared from AT1a-293T as described previously (Usui et al., 2000; Zhou et al., 2001). 500 μg proteins of the membranes and 10 μg proteins of His_6-RGS protein were incubated in buffer A [20 mM HEPES (pH 8.0), 500 mM NaCl, 3 mM DTT, 10 mM imidazole, 6 mM $MgCl_2$ and Complete™], with 100 μM GDP in the absence or presence of 30 μM AlF_4^-, or with 100 μM GTPγS, at 4 °C for 1 h. The mixture was solubilized with 1% cholic acid at 4 °C for 1 h. After centrifugation at 20,000 × g at 4 °C for 1 h, Ni^{2+}-NTA agarose beads were added to the supernatants and the mixture was incubated for 1 h. The beads were washed with appropriate buffer A supplimented with 0.1% $C_{12}E_{10}$. The proteins bound to Ni^{2+}-NTA agarose were separated by 12% of SDS-PAGE and transferred to polyvinylidene difluoride (PVDF) membranes. Immunoblotting was performed using anti-Gαs, Gαq/11, Gαi3, Gαi2, and Gαo Abs followed by peroxidase-conjugated goat anti-rabbit IgG Ab. Chemiluminescence reagent was used for detection of immunoreactivity. Intensity of chemiluminescence was quantified with a LAS-1000 luminescent image analyzer (Fuji Photo Film Co.).

Binding experiments of C2 domain and Gα subunits

AT1a-293T cells were cotransfected with Gα subunits and GST-tagged C2 domain of C2-RGS or PLC-β1, using Lipofectamine reagent and Plus reagent. Thirty hours after transfection, cells were pelleted and homogenized by 50 mM HEPES buffer (pH 7.4) containing Complete™. One mg of the cell suspension was incubated in the buffer B [20 mM HEPES (pH 8.0), 100 mM NaCl, 3 mM DTT, 6 mM $MgCl_2$, 0.1% $C_{12}E_{10}$, Complete™, and 0.2 mM phenylmethanesulfonyl fluoride (PMSF)] with 100 μM GDP in the absence or presence of 30 μM AlF_4^-, or with 100 μM GTPγS. After 1 h incubation, the mixture was solubilized by incubating with 1% cholic acid over night at 4 °C. After centrifugation at 20,000 × g for 1 h, glutathione-sepharose beads were added to the supernatant and the mixture was incubated for 1 h at 4 °C. After separation, the sepharose beads were washed with appropriate buffer B and subjected to SDS-PAGE and immunoblotting as described above.

GAP assay

Gαi3 (0.5 μM) protein was loaded with [γ-^{32}P]GTP (0.25 μM) in buffer C [50 mM Na-HEPES (pH8.0), 1 mM DTT, 5 mM EDTA and 0.1% $C_{12}E_{10}$] for 15 min at 25 °C, and then the temperature was lowered to 0 °C for 5 min. Before initiation of GTP hydrolysis, an aliquot (20 μl) of the mixture was mixed with 380 μl of 5% (wt/vol) charcoal in 50 mM NaH_2PO_4 plus 5 μl of starting solution. GTP hydrolysis reactions were initiated at 0 °C by adding $MgSO_4$ (12.5 mM) and unlabeled GTP (0.25 mM) with RGS protein (0.27 μM) or the buffer alone as control. Aliquots (25 μl) of the reaction mixture were withdrawn at the indicated times, and the reaction was stopped by addition of 380 μl of 5% (wt/vol) charcoal in 50 mM NaH_2PO_4. An aliquot (200 μl) of the supernatant containing ^{32}Pi released was counted by a liquid scintillation counter.

Results

Structural determination of a novel C. elegans RGS protein

Sequence analysis of a cDNA clone, yk534810 revealed that the predicted protein termed C2-RGS consists of 782 amino acid residues (GenBank accession No. AB080201). Based on the genome sequence of *C. elegans* (The *C. elegans* Sequencing Consortium, 1998), we found that the coding region for C2-RGS contains 14 exons and spans approximately 12 kb of the genome sequence of *C. elegans* cosmid F56B6 as indicated in Fig. 1. C2-RGS contains a C2 domain (amino acid residues 260–391) and an RGS domain (amino acid residues 635–763).

RGS domain of C2-RGS was found to be homologous to the conserved RGS domains of mammalian RGS proteins (Fig. 2A). RGS domain of C2-RGS is 48%, 47%, 46% and 42% identical to those of human RGS8, RGS3, RGS4 and RGS5, respectively, and less homologous to a *C. elegans* RGS protein, EGL-10 (32%).

C2 domain of C2-RGS, which has type I topology, showed much lower homology to known C2 domains (<27%) (Fig. 2B). Typical C2 domains of the Ca^{2+}-dependent type have four to six aspartic acid residues, in two or more Ca^{2+} binding loops at the apex of the folds formed by the eight-stranded β-sandwiches (Nalefski and Falke, 1996), whereas many C2 domains of the Ca^{2+}-independent type lack aspartic acid residues for Ca^{2+} binding. C2 domain of C2-RGS has only one aspartic acid and one glutamic acid residues in the relevant loops (Fig. 2B), suggesting that this C2 domain belongs to Ca^{2+}-independent type.

Effects of RGS domain and C2 domain on ET-1-induced Ca^{2+} responses

To reveal the function of C2-RGS and the role of C2 domain and RGS domain in the function, we prepared three mutants only with each of the domain and three deletion mutants, as indicated in Fig. 3. In this study, we used AT1a-293T cells, which have endogenous ETA receptors (Zhou et al., 2001). ETA receptor couples with Gαq/11, activates PLC-β, and increases intracellular Ca^{2+} concentrations.

Each of the full-length protein of C2-RGS or the mutants was expressed transiently in AT1a-293T cells at nearly the same expression level of the proteins, and effects of the expressed protein on ET-1-induced Ca^{2+} responses were analyzed. The full-length protein of C2-RGS strongly suppressed Ca^{2+}

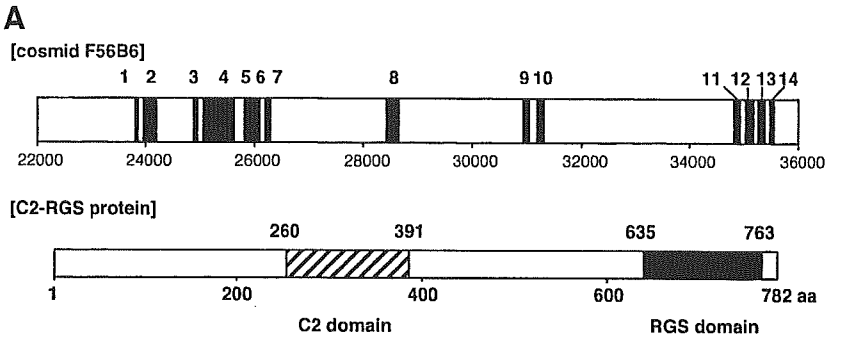

B

```
MTYTVRTKTKGLEALIRRAPVCGIAAQAVRRQILMNQQHEPNVLGNNKKVYQTFGSTPQL  60
ANERHKEMYSQIRRGDDSSFRSRDRFVPPRRPRMGYGSSDLSAIEEMSPIRSSTYSSSSE 120
AHRLSSLRAQTEWKPQLTSTTTSFQPLSPMNHHDKENGPFKAPMSPVCSSTPRSQRMYRK 180
NPKYRRQFGSSLQLSESRLEESTSQESERAVTPESWMEHNNENEHPDQMMFAKPKQGSFP 240
RPEAFGLDNAYAKHKDIRGIIFLSMSLCGRRLTLNVQNAAYFCSAARPTSVCSYVSAVLC 300
HRPSSQSSSSSRQYRQRPDECYRTRLVTNCNSPSFDESFYFTFSENCVRDLLIVTVYEMD 360
SNNAEKKRILGCMTFPVSRILKKASQVVGDPFPHYRRQDPMEDVEINNEGFFLLNKDQGR 420
KQNFPQRKVRRQTFYEDPAFTGVSSAGSSVISNNTGGQMTMASPRLSVPNELTMGDYYRS 480
TGSSDMRGRSTNNLLDYTSASSSTNGSAGGPEKLKLHRATLPSITTTTSENNSDDAKSLS 540
PEQSPTDHHFLCPDDNGGVYGAGPAHSAIKKSSVRRAASFTFSPKHSSSKTNLRQLNGRE 600
EDKEKKRFLGPISRTLSYLRSKMDLALSTSSLYPSRDDVRQWEISFESLLNNKFGCALFR 660
QFLKKEFSDENMDFWLECEEFKKMKDGKKSTTQKAIEIYSEFVAEHSPKEVNLDSDTRAA 720
TKAAVEAGCKPDTFALAQSRVEQLMSKDSYRRFLRDRLFLDLLESYEITDKEDKPSSSKD 780
KN 782
```

Fig. 1. A. Genomic organization of the coding region of C2-RGS. The gene of C2-RGS contains 14 exons and spans approximately 12 kb from ~ 24000 to ~ 36000 on the genome sequence of *C. elegans* cosmid F56B6. C2-RGS protein consists of 782 amino acid residues. B. The deduced amino acid sequence of C2-RGS (GenBank accession number: AB080201). C2 domain (amino acid residues 260–391) and RGS domain (amino acid residues 635–763) are underlined.

transients induced by ET-1 (0.1 nM–1.0 μM), by approximately 40%, and RGS domain suppressed them moderately by approximately 30% (Fig. 4A). Unexpectedly, a long form of C2 domain (C2L, amino acid residues 253–436) also suppressed the Ca^{2+} responses by 20%. Another form of C2 domain (amino acid residues 259–391, which is a region corresponding to the C2 domain) also showed a similar inhibitory effect (data not shown). A short form of C2 domain (C2S, amino acid residues 271–388, which is a region assigned to the C2 domain by SMART (*S*imple *M*odular *A*rchitecture *R*esearch *T*ool) program) lacking strand 1, also showed an inhibitory effect, which was comparable to, or slightly weaker than that of C2L (Fig. 5A and B). The inhibitory effects of the RGS, C2L and C2S were dependent on the DNA doses used for their transient expression, as shown in Fig 5.

When a mutant protein lacking C2 or RGS domain was expressed, C2 domain-deleted (ΔC2) or RGS domain-deleted (ΔRGS) protein suppressed ET-1-induced Ca^{2+} transients, similar to RGS or C2 domain proteins, respectively. A mutant lacking both C2 and RGS domains (ΔC2ΔRGS) did not show any effects (Fig. 4B).

Since these results demonstrated that all C2 domain-containing proteins of C2-RGS suppress ET-1-induced Ca^{2+} responses, we tested the possibility that another C2 domain also regulates Gαq-mediated Ca^{2+} signaling negatively. When C2 domain of human PLC-β1 (PLC-C2) was transiently expressed, it

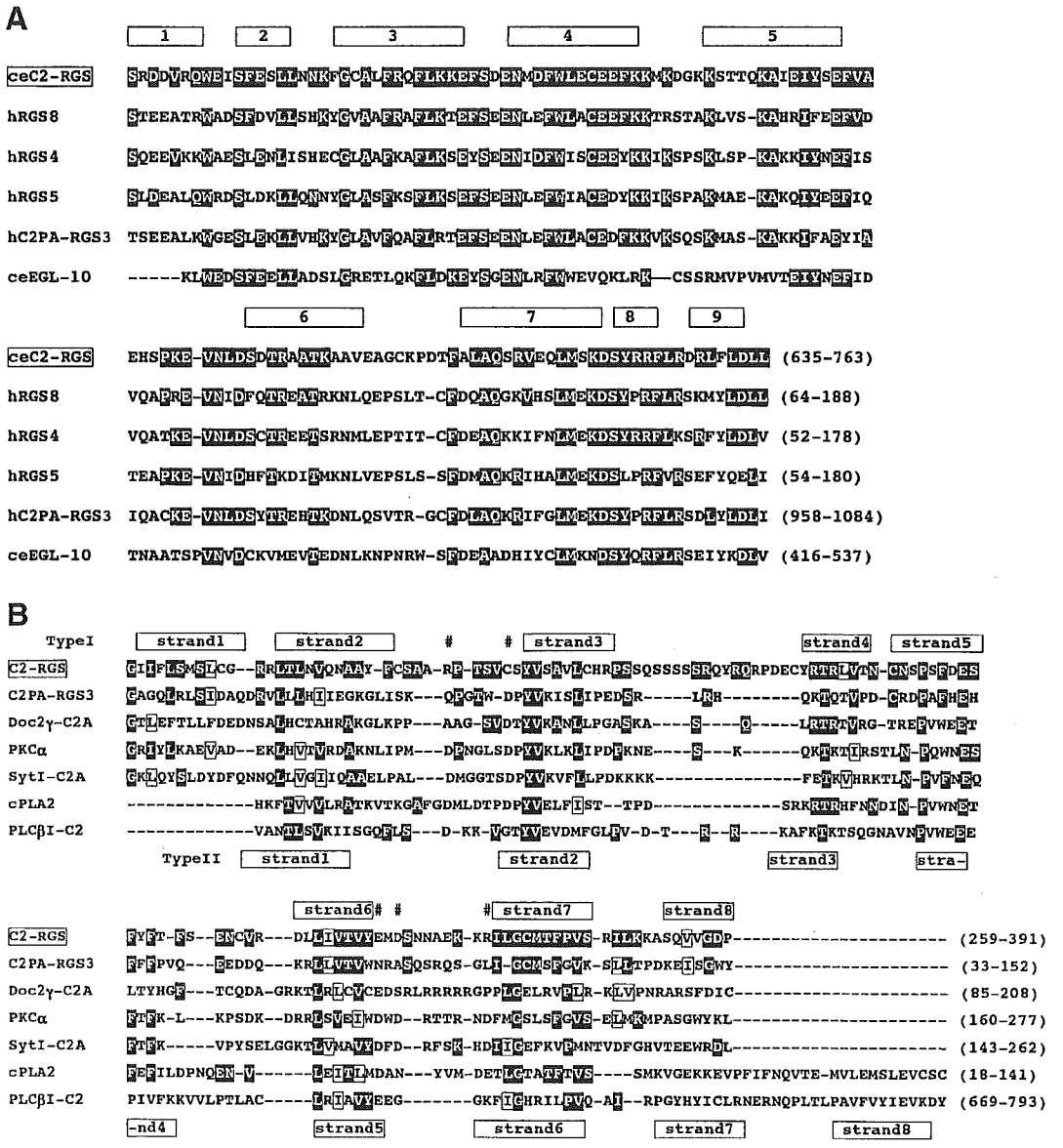

Fig. 2. A. Sequence alignment of RGS domains for *C. elegans* and human RGS proteins. Conserved amino acids are highlightened in black. Regions of the nine α helices found in RGS4 are indicated. B. Sequence alignment of C2 domains for *C. elegans* and mammalian C2 proteins. Conserved and similar amino acids are shown highlightened in black and boxed, respectively. The sharps (#) indicate five conserved aspartic acid residues essential for Ca^{2+} binding in synaptotagmin I C2A. The secondary structures (strand 1 ~ strand 8) of type I and type II topologies are schematically shown. Note that C2 domain of ceC2-RGS contains only one of five aspartic acid residues. ce, *C. elegans*; h, human; hc, human cytosolic; m, mouse; syt, synaptotagmin; PKC, protein kinase C.

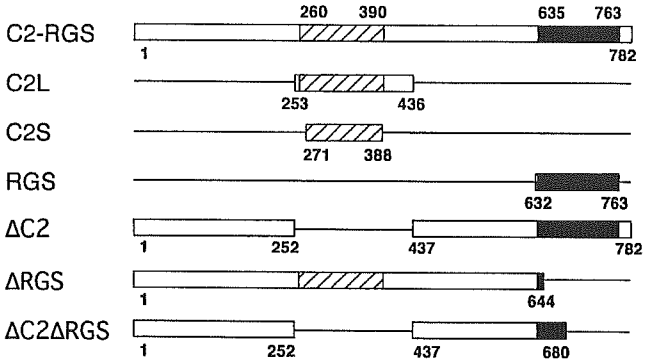

Fig. 3. Schematic representation of C2-RGS and its mutants used in this study. C2-RGS, the full-length form (1-782) of C2-RGS; C2L, a long form (253–436) of C2 domain; C2S, a short form (271–388) of C2 domain; RGS, a fragment (632–763) with RGS domain; ΔC2, C2-RGS lacking C2 domain (253–436); ΔRGS, C2-RGS lacking RGS domain (645–782); ΔC2ΔRGS, C2-RGS lacking both C2 domain (252–436) and RGS domain (681–782).

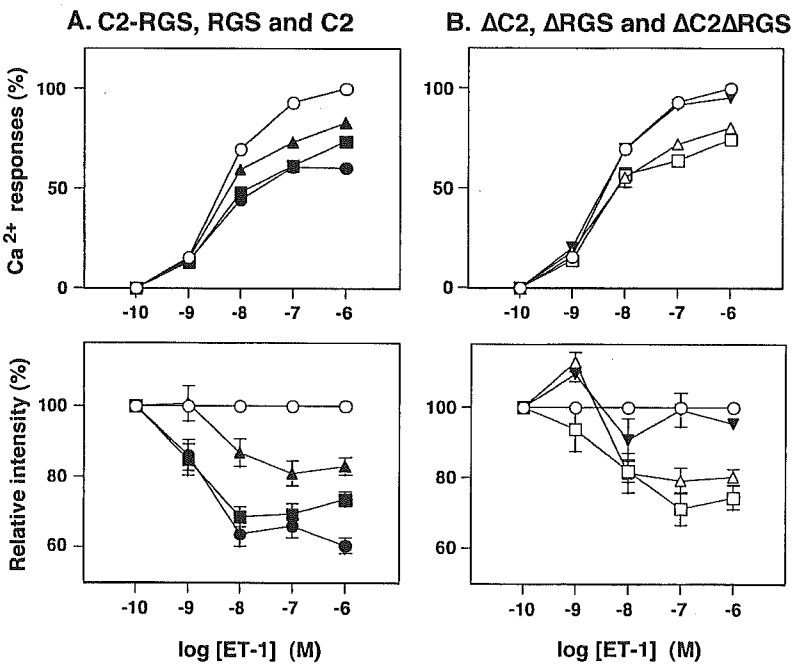

Fig. 4. Inhibition of intracellular calcium ($[Ca^{2+}]i$) responses to ET-1 by C2-RGS and its mutants. A. Upper graph, $[Ca^{2+}]i$ responses to various concentrations of ET-1 in AT1a-293T cells transfected with the full-length form of C2-RGS (closed circles), RGS domain (closed squares), C2L (closed triangles) or the empty vector (pCMV6c) (open circles). Responses were normalized as percentages of the responses to 1 μM ET-1 in cells transfected with the empty vector. Lower graph, relative inhibitory effects of C2-RGS, RGS domain, or C2L. Responses were normalized as percentages of those induced by each concentration of ET-1 in cells transfected with the empty vector. Results were means ± SEM of 5–11 experiments. B. $[Ca^{2+}]i$ responses to ET-1 in AT1a-293T cells transfected with ΔC2 (open squares), ΔRGS (open triangles), ΔC2ΔRGS (inverted closed triangles) or the empty vector (open circles). Results were means ± SEM of 5–11 experiments.

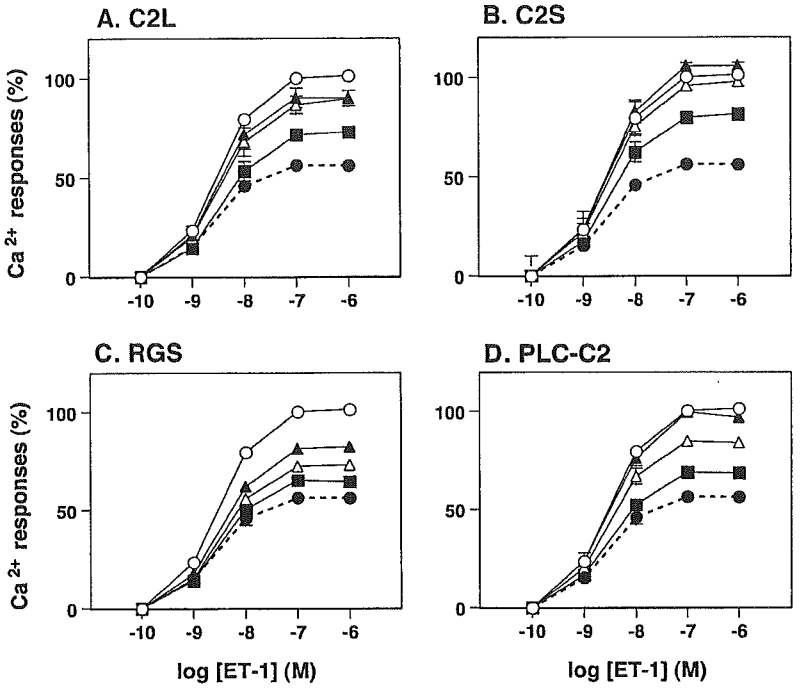

Fig. 5. Relationship between inhibitory effects of various C2 domains and RGS domain and the DNA doses used for transfection. $[Ca^{2+}]i$ responses induced by increasing concentrations of ET-1 were measured in AT1a-293T cells transfected with three DNA doses (0.2 μg (closed triangles), 0.6 μg (open triangles) and 2.0 μg (closed squares)/6 cm dish) of C2L, C2S, RGS, and PLC-C2. They were compared to those in cells transfected with 2.0 μg/6 cm dish of the empty vector (pCMV6c) (open circles) or the full-length form of C2-RGS (closed circles). In each case, total amounts of transfected DNA were adjusted to 2.0 μg/6 cm dish with pCMV6c. Responses were normalized as percentages of those induced by 1 μM ET-1 in cells transfected with the empty vector. Results were means ± SEM of 5–8 experiments.

also suppressed the Ca^{2+} responses, as effectively as, or slightly less potently than C2L. The inhibitory effect was also dependent on the expression level (Fig. 5D).

Binding of RGS domain and C2 domain to Gα subunits

Binding property of RGS domain to mammalian Gα subunits was studied using His_6-RGS domain and membranes of AT1a-293T cells. His_6-RGS domain bound to Gαi2, Gαi3, Gαo, and Gαq/11, but not to Gαs, only in the presence of GDP/AlF_4^-, but not in the absence of GDP/AlF_4^- (Fig. 6). The same results were obtained by using GST-RGS (data not shown).

Since C2 domains of C2-RGS and PLC-β1 showed inhibitory effects on Ca^{2+} signaling, we examined whether they associate with Gα subunits. In binding experiments, GST-C2S was used in place of C2L, because of difficulty to prepare GST-C2L in a soluble form. The results showed that GST-C2S bound strongly to Gαq and weakly to Gαs, Gαi3 and Gαo, which were coexpressed transiently with GST-C2S (Fig. 7A). The binding of C2 domain to Gαq was roughly 10-fold tighter than that to Gαi/o subunits, estimated from the intensity of the band of each Gα subunit bound to GST-C2S, relative

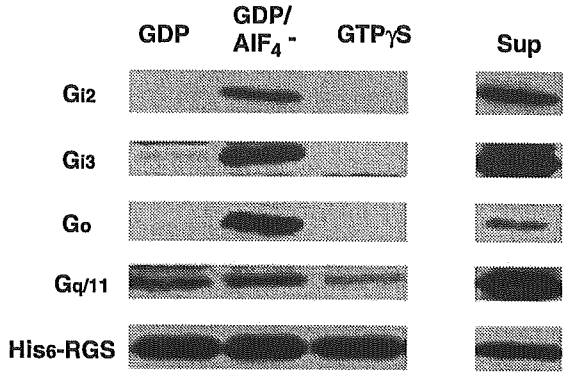

Fig. 6. Binding of recombinant His_6-RGS domain to Gα subunits in AT1a-293T cells. One two hundredth of the supernatants (Sup) and one fourth fraction of the affinity precipitates adsorbed to Ni^{2+}-NTA agarose in the presence of GDP, GDP/AlF_4^- or GTPγS, were separated by 12% of SDS-PAGE, and immunoblotting was performed for Gα subunits using rabbit anti-Gα Abs. This assay was repeated three times and a representative result is shown.

to that of the total amount of the respective Gα subunit. GST-PLC-C2 also bound strongly to Gαq, and not to Gαi3 and Gαo subunits (Fig. 7B). A unique feature of the binding of these C2 domains was that they bound to Gαq subunit almost equally under all the experimental conditions used; the presence of

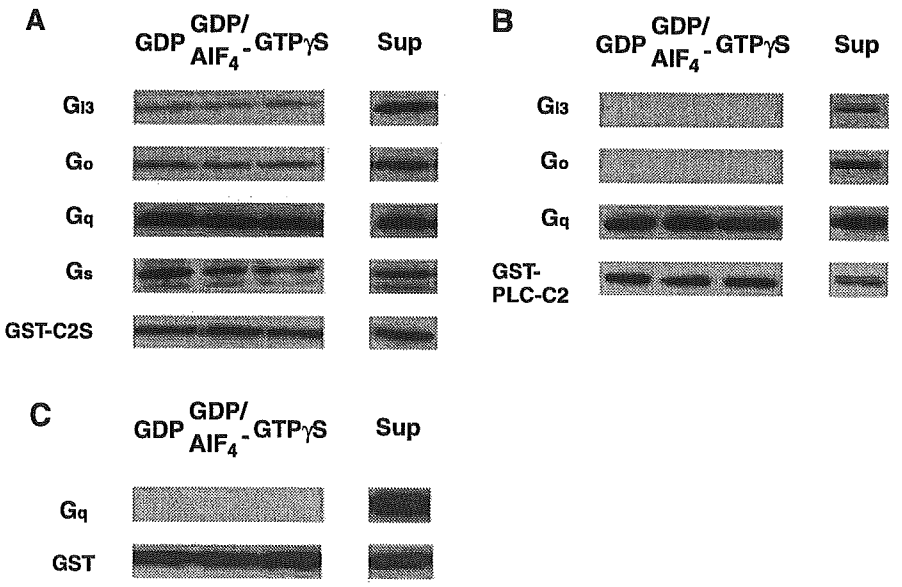

Fig. 7. Binding of GST-C2S and GST-PLC-C2 to Gα subunits. A. Binding of GST-C2S to Gα subunits. AT1a-293T cells were cotransfected with GST-tagged C2 domain of C2-RGS and each Gα subunit using Lipofectamine reagent and Plus reagent. One two hundredth of the supernatants (Sup) and one fourth fraction of the affinity precipitates adsorbed to glutathione-sepharose beads in the presence of GDP, GDP/AlF_4^- or GTPγS, were separated by 12% of SDS-PAGE, and immunoblotting was performed for Gα subunits using rabbit anti-Gα Abs. This assay was repeated three times and a representative result is shown. B. Binding of GST-PLC-C2 to Gαq subunit. Experiments were performed as described in A, using GST-PLC-C2. C. Binding of control GST protein to Gαq subunit.

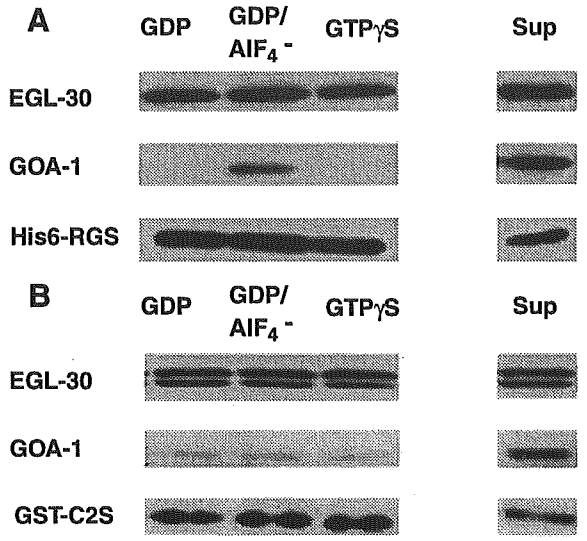

Fig. 8. Binding of His_6-RGS and GST-C2 to EGL-30 and GOA-1. A. Binding of recombinant His_6-RGS to membranes of AT1a-293T cells transfected with EGL-30 or GOA-1. One two hundredth of the supernatants (Sup) and one fourth fraction of the affinity precipitates adsorbed to Ni^{2+}-NTA agarose in the presence of GDP, GDP/AlF_4^- or GTPγS, were separated by SDS-PAGE. Immunoblotting was performed using anti-c-myc. B. Binding of GST-C2S to EGL-30 or GOA-1. AT1a-293T cells were cotransfected with GST-C2S and EGL-30 or GOA-1. One two hundredth of the supernatants (Sup) and one fourth fraction of the affinity precipitates adsorbed to glutathione-sepharose beads in the presence of GDP, GDP/AlF_4^- or GTPγS, were separated by SDS-PAGE. Immunoblotting was performed using anti-c-myc Ab. This assay was repeated three times and a representative result is shown.

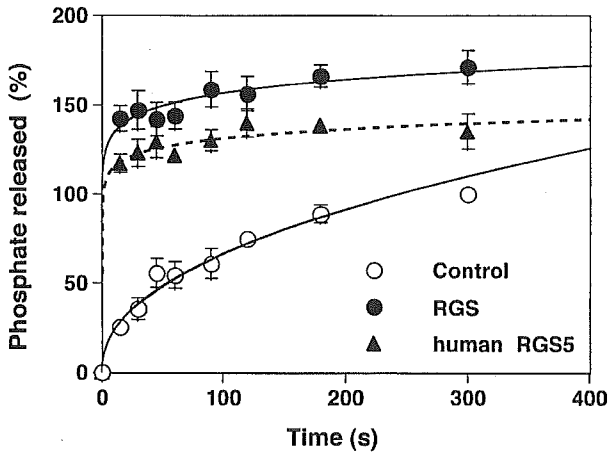

Fig. 9. GAP activity of RGS domain of C2-RGS and RGS5 towards Gαi3. The GTPase activity of Gαi3 was determined in the presence of RGS domain of C2-RGS (closed circles) or human RGS5 (closed triangles), or in their absence (open circles), as described in the section of "Methods". Values of ^{32}Pi released were normalized as percentages of those in the absence of RGSs at 300 sec. Results were means ± SEM of 5–7 experiments.